ACS OMEGA

Open Access

http://pubs.acs.org/journal/acsodf

Article

Modified Cellulose for Adsorption of Methylparaben and Butylparaben from an Aqueous Solution

Yaned Milena Correa-Navarro,* Juan David Rivera-Giraldo, and Julio Andrés Cardona-Castaño

Cite This: *ACS Omega* 2024, 9, 30224−30233

Read Online

ACCESS | Metrics & More | Article Recommendations | Supporting Information

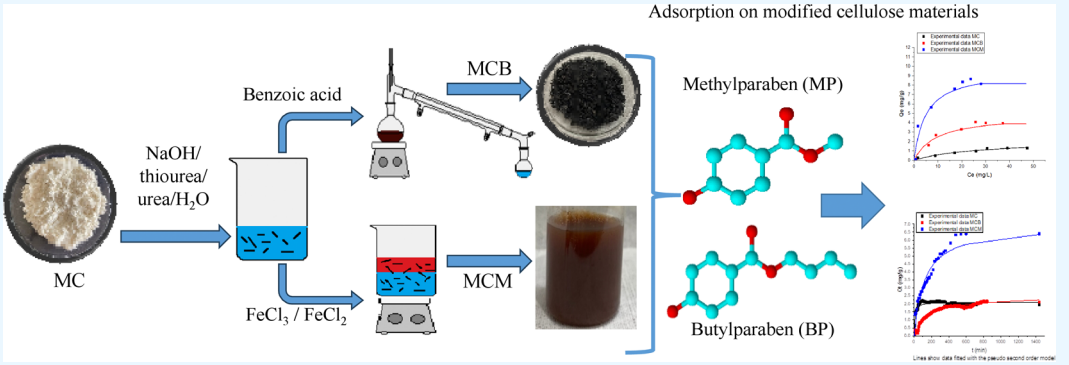

ABSTRACT: Emerging contaminants are chemical products that are found in low concentrations, are not regulated by environmental norms, and cause health effects. Among this group of contaminants are parabens, a family of *p*-hydroxybenzoic acid esters used as preservatives in cosmetics, pharmaceuticals, and food products. Recent research describes parabens as endocrine disruptors that can cause health alterations. Some of the best alternatives for pollutant removal include the adsorption process, which can use materials that are inexpensive, abundant, and susceptible to modifications. In this sense, cellulose can be an option for obtaining materials that can be used in the removal of contaminants. This research investigates the synthesis of benzoic cellulose (MCB) and magnetic cellulose (MCM) as well as its use as an adsorbent for the removal of methylparaben (MP) and butylparaben (BP) from water. Likewise, physicochemical characterization, including Fourier transform infrared (FTIR), scanning electronic microscopy (SEM), energy-dispersive spectroscopy (EDS), X-ray diffraction (XRD), and thermogravimetric analysis (TGA), for both cellulose materials was carried out. Moreover, pseudo-first-order, pseudo-second-order, Elovich, Weber, Morris, and Boyd models were used to investigate the adsorption kinetics. As a result, the pseudo-second-order model was favorable for both modified cellulose and the two parabens assayed. Finally, Freundlich, Langmuir, and Sips adsorption isotherm models were investigated; the Langmuir model was the best for the adsorption isotherm data. The adsorption of methylparaben and butylparaben was in the following order: MCM > MCB. The maximum adsorption capacity of MP and BP for MCM was 9.58 and 12.03 mg g^{-1}, respectively. For instance, the results showed that the modified cellulose adsorbed the parabens physically, which could involve electrostatic attraction, hydrogen bonding, $\pi-\pi$ bonding, and hydrophobic interactions.

INTRODUCTION

Parabens are alkyl esters of *p*-hydroxybenzoic acid with alkyl substituents such as methylparaben (MP), ethylparaben (EP), propylparaben (PrP), and butylparaben (BP).[1−3] They are colorless, odorless, and chemically stable over a wide pH range.[4] Some parabens have antibacterial and antifungal activities due to their ability to alter the cell membrane and intracellular proteins and cause a change in the enzymatic activity of microbial cells.[3] Parabens are used as synthetic preservatives in cosmetics, food, pharmaceuticals, and personal care products.[5] For instance, at the food level, they are used as antimicrobial preservatives in baked goods, fats and oils, condiments, sugar substitutes, coffee extracts, fruit juices, pickles, sauces, soft drinks, and dairy products.[1,6]

Parabens are recognized as endocrine-disrupting chemicals (EDCs) that can mimic, antagonize, or modify natural hormone levels in the body.[7,8] In this way, the functions of the endocrine system can be altered; therefore, the health, development, and reproduction of living beings are affected.[9] In fact, even at low concentrations, parabens can cause different effects, such as gestational diabetes,[10] infertility,[11] and

Received: December 23, 2023
Revised: June 14, 2024
Accepted: June 18, 2024
Published: July 4, 2024

https://doi.org/10.1021/acsomega.3c10304
ACS Omega 2024, 9, 30224−30233

breast cancer.[12] The maximum allowable concentration of parabens in Europe is 0.4% for individual parabens and 0.8% for a mixture of parabens.[13] In Colombia, the Instituto Nacional de Vigilancia de Medicamentos y Alimentos (Invima), in February 2017, began to ban cosmetic products containing within their formulations long-chain parabens such as isopropylparaben, isobutylparaben, phenylparaben, benzylparaben, and pentylparaben.[14]

As a consequence of their great industrial uses, parabens are released and detected in surface water, industrial wastewater, soils, and reservoirs. For example, in surface wastewater, MP and PrP have been found at 170.9 and 52.1 μg L^{-1}, respectively. In addition, in water resources, EP and BP were detected at 30.5 and 19.9 μg L^{-1}, respectively.[8]

Researchers have reported parabens remotion in water samples using adsorbents.[1] As an example, magnetic nanoparticles with a phenyl group were used for the removal of MP, EP, and PrP and displayed adsorption capacities of 0.6015, 3.2862, and 3.5421 mg g^{-1}, respectively.[15] In addition, micro- and mesoporous silica synthesized from coal fly ash were used for the adsorption of parabens in aqueous media.[16]

The use of low-cost adsorbents has been investigated as an alternative to the current expensive methods for the removal of contaminants from aqueous solutions. Previous works reported that unmodified cellulose has low adsorption capacity and variable physical stability.[17] However, chemical modification of cellulose can be performed to achieve adequate structural durability and efficient adsorption capacity for organic and inorganic pollutants.[18] The hydroxyl groups present on the surface and the relatively large specific surface area of cellulose provide abundant active sites for modification by various chemical reactions.[19] In this way, properties of cellulose, such as its hydrophilic or hydrophobic character, elasticity, adsorption, and ion exchange capacity, can be realized.[17]

In this study, the aim was to synthesize magnetic cellulose (MCM) and benzoic cellulose (MCB) composites. Afterward, a comparative study of the removal of methylparaben and butylparaben from aqueous solutions by adsorption onto both adsorbents was carried out.

MATERIALS AND METHODS

Reagents. Methylparaben (MP) and butylparaben (BP) were purchased from Sigma-Aldrich. Table S1 shows some properties of MP and BP. Microcrystalline cellulose (MC), urea ($CO(NH_2)_2$), thiourea ($SC(NH_2)_2$), sodium hydroxide (NaOH), benzoic acid (BA), ferrous chloride tetrahydrate ($FeCl_2{\cdot}4H_2O$), ferric chloride hexahydrate ($FeCl_3{\cdot}6H_2O$), sodium chloride (NaCl), and all other reagents were of analytical grade and were supplied by Merck.

Microcrystalline Cellulose Solution (MCS). Microcrystalline cellulose solution was prepared employing the methodology of Periyasamy et al., with some modifications.[20] Specifically, in our procedure, 4.0 g of microcrystalline cellulose was dissolved in 200 mL of a NaOH/thiourea/urea/H_2O (8:6.5:8:77.5) solution; consequently, this mix was stirred for 20 h at −5.0 °C to form a homogeneous microcrystalline cellulose solution (MCS).

Cellulose Modified with Benzoic Acid (MCB). We used a variation of Espino-Pérez et al. procedure[21] to obtain cellulose with benzoic acid (MCB). In fact, in our procedure, the pH of 100 mL of the microcrystalline cellulose solution (MCS) was adjusted to 4.0 with concentrated sulfuric acid. Subsequently, an excess of benzoic acid (10 equiv according to the dry weight of MCS) was slowly added, and the solution was placed in a closed distillation system for 20 h at 80.0 °C to achieve the MC esterification. After the reaction, the MCB product was purified by removing unreacted BA by filtration and adding a large excess of hot water (5 washes) and ethanol (3 washes). Finally, the MCB material was oven-dried at 60 °C.

Magnetic Cellulose (MCM). Magnetic cellulose denoted as MCM was prepared employing the method used by Periyasamy et al., with some changes.[22] Initially, the MCS pH was adjusted to 10.0; subsequently, this solution was stirred vigorously using a magnetic plate. Afterward, 10 mL of a solution containing 1.85 mmol of $FeCl_2$ and 3.7 mmol of $FeCl_3$ was gradually added to MCS, maintaining the pH at 10.0. The resulting dark brown suspension was kept for 24 h. After that, the resulting slurry was separated and washed with distilled water to a neutral pH, and a final wash was performed with ethanol. This material was a magnetic compound, named MCM.

Characterization of Modified Cellulose. The modified cellulose obtained through the different methods previously described was characterized by various techniques. The techniques used are described as follows: The morphology of cellulose was obtained using a scanning electron microscope (SEM) with an energy-dispersive spectrometry (EDS) detector (QUANTA 250 FEI). To analyze, the samples were coated with gold. Fourier transform infrared spectroscopy (FTIR) was performed using a Shimadzu IRTracer-100 FTIR spectrophotometer. All samples were mixed with KBr to produce a homogeneous disk. After that, the samples were deposited separately in the diffuse reflectance cell of the infrared equipment, and spectra were recorded in the range of 4000−400 cm^{-1}.[23,2423,24] Thermogravimetric analysis (TGA) was performed in a Hitachi, TGA/STA7200 system under a nitrogen atmosphere. The heat rate was 10 °C min^{-1}, and the heating range was 37−950 °C.[25] The X-ray diffraction (XRD) data were obtained using a PANalytical Empyrean model. The samples were measured in a conventional Bragg−Brentano optical configuration with a copper anode X-ray generator tube (λ = 1.54 Å). XRD patterns were obtained in the Bragg angle range (2θ) from 5 to 70°.

Adsorption Assays. 5.0 mL of methylparaben (MP) and butylparaben (BP) solutions was put in vials that contained a preweighed amount of modified cellulose; subsequently, cylindrical glass vessels were placed in a controlled orbital shaker at 150 rpm. Parameters such as time (0−48 h) and initial MP or BP concentration (1.0−40.0 mg L^{-1}) were evaluated. In all assays, the MP or BP concentration that remained in the supernatant was determined using a UV spectrophotometer (UV-1600, MAPADA) at λ = 255 nm. The adsorption capacity of modified cellulose at any time (Q_t, mg g^{-1}) and at equilibrium time (Q_e, mg g^{-1}) was calculated from eq 1. All studies were carried out in triplicate.

$$Q_e = \frac{V(C_0 - C_e)}{W} \quad (1)$$

where C_0 is the initial concentration of MP or BP (mg L^{-1}), C_e is the concentration of MP or BP at equilibrium, V (L) is the volume of MP or BP solution, and W (g) is the dry mass of the modified cellulose used.[23]

Adsorption Isotherms. Adsorption isotherms are important in the development of the adsorption process because they allow the adsorbent/adsorbate interaction to be

https://doi.org/10.1021/acsomega.3c10304
ACS Omega 2024, 9, 30224−30233

estimated. In this study, the adsorption capacity of modified cellulose at any time (Q_t, mg g^{-1}) and at equilibrium time (Q_e, mg g^{-1}) was calculated employing three isotherm models: Langmuir, Freundlich, and Sips (Table S2).[26] Actually, these models allow us to study and elucidate the adsorption behavior of MP and BP on modified cellulose materials.

Kinetic Study. To determine the time required to reach adsorption equilibrium, 9.0 mg of the modified cellulose materials (MCB and MCM each separately) was put in contact with 3.0 mL of a solution of MP at 15.0 mg L^{-1} or BP at 25.0 mg L^{-1}. Adsorption kinetics were monitored for a total time of 24 h, employing a UV spectrophotometer (UV-1600, MAPADA) at λ = 255 nm. The adsorption capacity of the modified cellulose was calculated from eq 1, and the data were fitted with the kinetic models: pseudo-first-order, pseudo-second-order, Elovich, Boyd, and Weber−Morris (Table S2).[27]

Reuse Tests of Cellulosic Materials. To analyze the stability of the MCB and MCM adsorbents, the materials were washed at the end of each test. Then, the materials were separated from the solution (by decanting), washed three times with hot water and twice more with distilled water, and finally dried at 60 °C for 6 h before being used in a new cycle.[28]

Statistical Analysis. Additionally, the quality of fitting the mathematical models was verified using the coefficient of determination (R^2), the sum of the squares of the error (SSE), the average relative error (ARE (%)), and the hybrid fractional error function (HYBRID). These equations are in Table S3, and the results are in Tables S4 and S6.[29]

RESULTS AND DISCUSSION

Physicochemical Characterization of the Cellulose Modified. Surface modification of cellulose through its hydroxyl groups has been used to improve its properties for increased applications of this material.[19,30] A diversity of chemical groups have been added to cellulose surfaces through reactions such as oxidation and acetylation.[31,32] In addition, the esterification of cellulose is an acylation process of hydroxyl groups employing carboxylic acid as an acylating agent under strong acid catalysis (Fischer esterification).[33,34] We adapted the procedure reported by Espino-Pérez,[21] using benzoic acid in acid catalysis and heating under reflux to obtain an

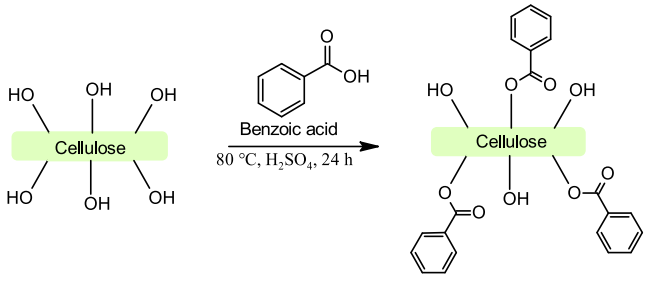

Figure 1. Cellulose modified with benzoic acid.

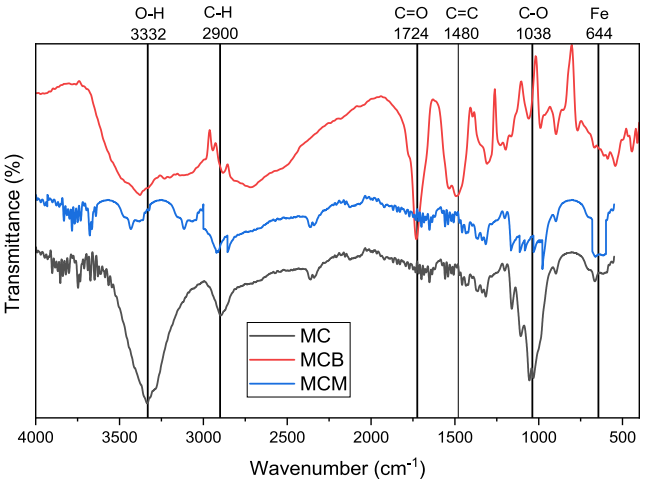

Figure 3. FTIR spectra of microcrystalline cellulose (MC), cellulose with benzoic acid (MCB), and magnetic cellulose (MCM).

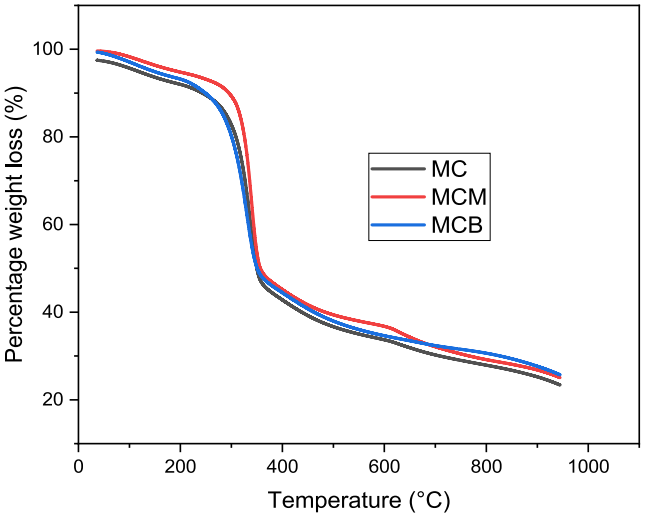

Figure 4. Thermogram of microcrystalline cellulose (MC), cellulose with benzoic acid (MCB), and magnetic cellulose (MCM).

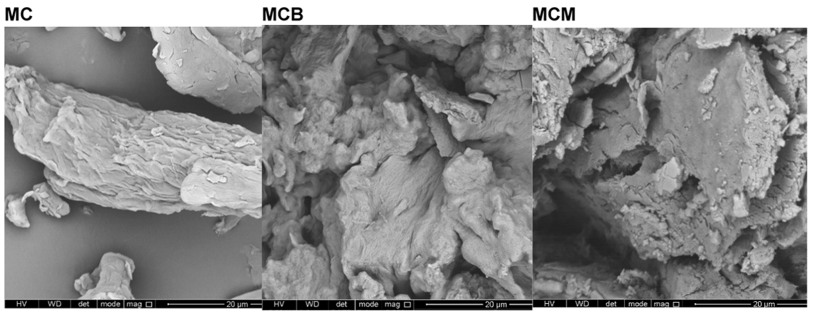

Figure 2. Micrographs of raw and modified cellulose: microcrystalline cellulose (MC), cellulose with benzoic acid (MCB), and magnetic cellulose (MCM).

https://doi.org/10.1021/acsomega.3c10304
ACS Omega 2024, 9, 30224−30233

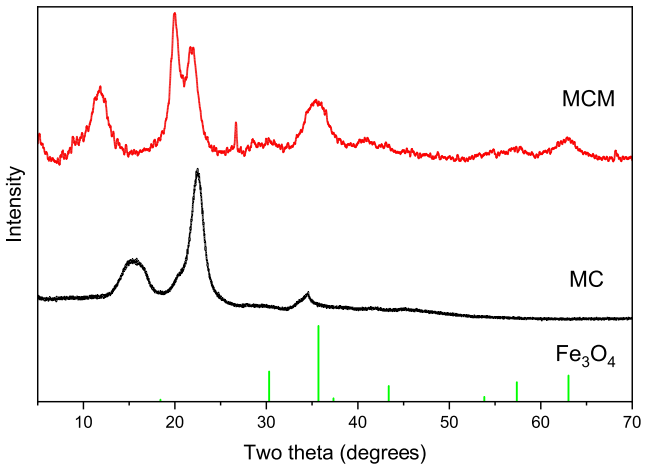

Figure 5. X-ray diffraction of microcrystalline cellulose (MC) and magnetic cellulose (MCM).

esterification reaction as shown in Figure 1. The employed method is in line with the principles of green chemistry: use of an aqueous suspension, nontoxic carboxylic acids, moderately low reaction temperature, reaction at ambient pressure, and the possibility of recovering the excess of reactants by solvent distillation.[25]

On the other hand, magnetic nanoparticles have been used to efficiently remove parabens, and various physical and chemical modifications have been used to improve the adsorption capacity of this material.[1] Some of them used matrices such as chitosan,[35,36] polymers,[17,37,38] carbon,[39] carbon nanotubes (CNT),[40] graphene oxide (GO),[41] metal oxides,[42,43] zeolites,[44] and metal−organic frameworks (MOFs).[45,46] In our study, magnetic nanoparticles were generated according to eq 2 and coated on cellulose.[20,47]

$$Fe^{2+} + 2Fe^{3+} + 8OH^- \rightarrow Fe_3O_4 + 4H_2O \quad (2)$$

Micrographs of the modified cellulose (Figure 2) showed different structures and morphologies depending on the chemical treatment employed. In general, the prepared cellulose displayed a heterogeneous surface, as expected the raw microcellulose (MC) has a smooth morphology with amorphous areas; similarly, the cellulose modified with benzoic acid (MCB) has a rough and irregular surface due to the hydrolysis influence that causes the degradation of cellulose fibers.[48,49] Moreover, magnetic cellulose (MCM) showed spherical particles, which is consistent with Zirak,[50] who reported that methyl cellulose coated with Fe_3O_4 had spherical nanoparticles.

The X-ray dispersive spectra (EDX) of MC showed a weight percentage of 73.07% C and 26.93% O, while MCB had values of 56.34% C and 43.66% O, which is evidence of a higher presence of oxygen, and this demonstrates that the cellulose was esterified with benzoic acid. Finally, the MCM material had a weight percentage of 55.46% C, 41.10% O, and 2.8% Fe, indicating the presence of magnetite on the surface of the microcellulose (Figure S1).

Figure 3 shows the FTIR spectra of MC, MCB, and MCM. The MC spectrum displayed the common peaks of cellulose: broad hydroxyl stretching at 3332 cm^{-1} and bending at 1610 cm^{-1}, the C−O signal at 1038 cm^{-1}, and a C−H stretching peak at 2900 cm^{-1}, respectively. On the other hand, the MCB spectrum showed a lower intensity peak at 3332 cm^{-1} assigned to hydroxyl stretching, while the peak at 1724 cm^{-1} was associated with carbonyl stretching of the acid, both absorptions confirming the conversion of the primary C6 hydroxyl to carboxyl from esterification with benzoic acid.[33] Furthermore, the peak at 1480 cm^{-1} was assigned to aromatic C═C groups.[23] Finally, the CMM spectrum shows a peak at 644 cm^{-1} signal that is associated with the stretching vibrations of the Fe−O bond,[50] which allows confirming the coating of the microcellulose with Fe_3O_4. As expected, the FTIR experiment showed that the chemical reactions employed were successful and that modified cellulose was achieved.

Thermograms of MC, MCB, and MCM are shown in Figure 4. TGA of all materials shows the first weight loss at 100−120 °C, which corresponds to the removal of physically adsorbed water, and the second weight loss, which occurs at 220−380 °C, is attributed to the decomposition of the organic structure of the microcellulose polymer. These results are in agreement with other authors.[21,25,50]

The changes in the crystal structure due to the modifications made to MC during the processing of the MCM material were determined from the XRD diffractogram of the pure MC and the composite MCM. The XRD pattern of MC in Figure 5 shows the typical structure of cellulose I with peaks at 2θ = 15.40° and 22.40, which are characteristic of crystalline cellulose and correspond to the diffraction lattice planes of (110) and (020), and this is consistent with Van et al. and Chen et al.[51,52] The characteristic XRD signals of Fe_3O_4 correspond to 2θ = 30.30, 35.69 43.38, 57.38, and 63.02°.[53] The processed MCM material showed signals at 2θ = 35.50, 57.34, and 63.00°, indicating the presence of Fe_3O_4 and corresponding to the diffraction lattice planes of (311), (440), and (511) (JCPDS card 01-075-0449), and similar to the results of previous works.[54,55] In addition, due to the alkaline treatment of the MCM material, the crystalline peak of MC (22.40°) split into two peaks located at 2θ = 20.02 and 21.80°, showing a typical structure of cellulose II. A shift of the MC peak from 15.40 to 11.78° is also recorded in the MCM characteristic of cellulose II. These values correlate favorably with Li et al. and Yue.[56,57]

Adsorption Kinetic. To determine the adsorption equilibrium time, we carried out dynamic adsorption assays of methylparaben and butylparaben on modified cellulose. The recorded experimental data were then fitted nonlinearly using pseudo-first-order, pseudo-second-order, and Elovich models. The effect of contact time (Figure 6a,6b) revealed that the adsorption capacity of parabens displayed an increase with the increase of time and reached the equilibrium state within 200 min for both parabens on MC and MCB. In addition, on MCM, the equilibrium state was reached within 600 min for both parabens. The single most striking to emerge from the kinetic data comparison was that it is possible that the MP and BP molecules interacted with the aromatic and hydroxyl groups on MCB and MC fast. In contrast, parabens interacted with coated Fe_3O_4-MC adsorbent through electrostatic forces, achieving removal of parabens in more time.

Table S4 shows values of the parameters obtained by the pseudo-first, pseudo-second, and Elovich models employed to evaluate adsorption kinetic data for methylparaben and butylparaben. These results offer powerful evidence that pseudo-second-order models were the best option for both MP and BP adsorption as they presented the highest R^2 values (0.9414−0.9977) and the lowest error function values. In addition, the values of $Q_{e\ cal}$ by the pseudo-second-order model

https://doi.org/10.1021/acsomega.3c10304
ACS Omega 2024, 9, 30224−30233

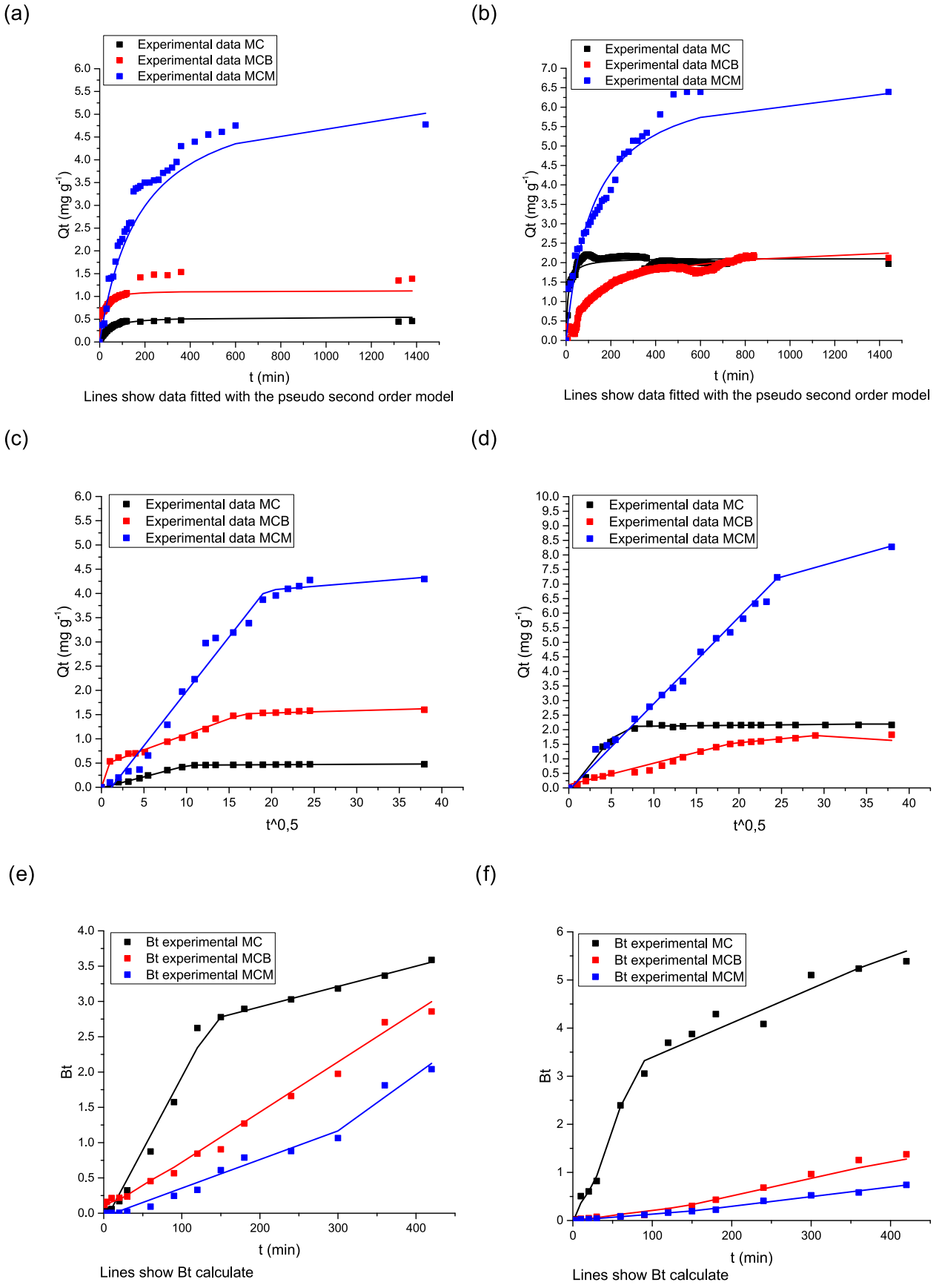

Figure 6. Graphs of kinetic models for methylparaben and butylparaben adsorption onto modified cellulose: (a, b) pseudo-second model; (c, d) Weber−Morris model; (e, f) Boyd model.

https://doi.org/10.1021/acsomega.3c10304
ACS Omega 2024, 9, 30224−30233

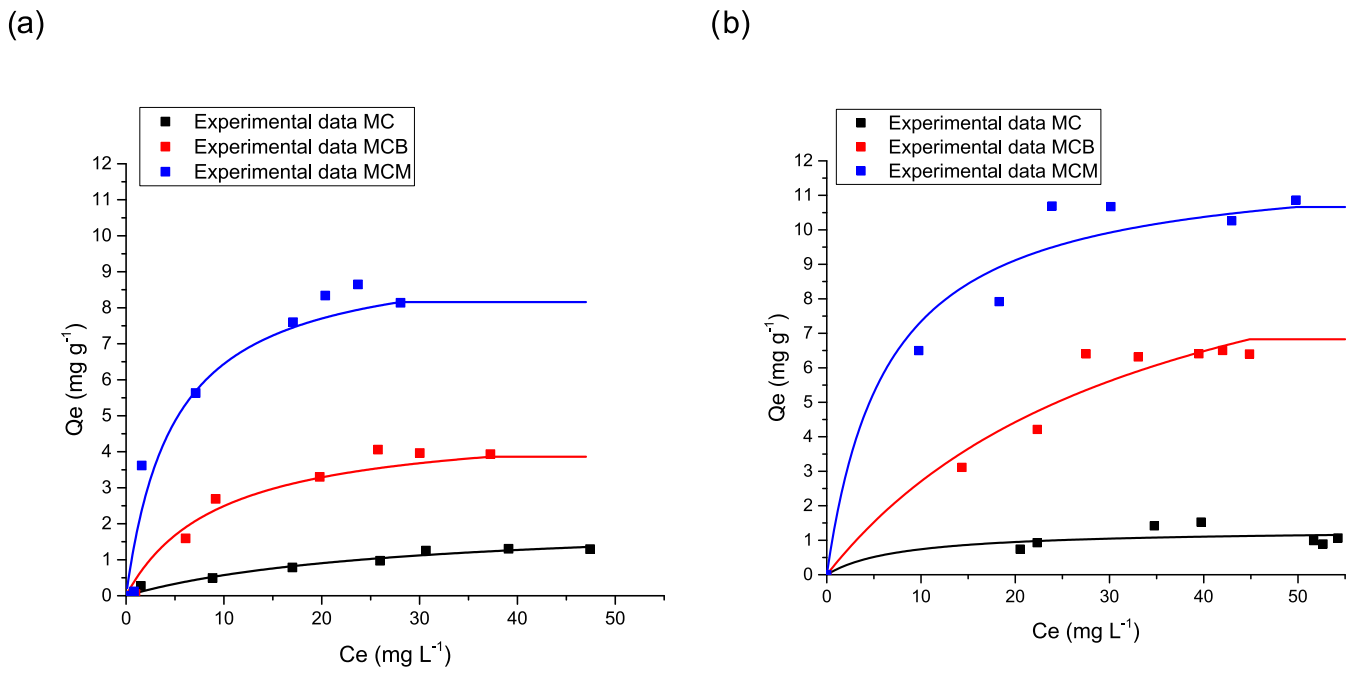

Figure 7. Adsorption isotherm onto modified cellulose at 20 °C of (a) methylparaben and (b) butylparaben (the lines show data fitted with the Langmuir model).

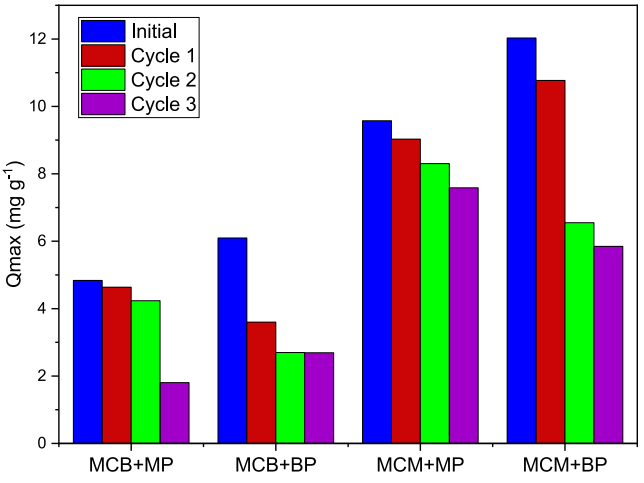

Figure 8. Adsorption performance of modified cellulose at 20 °C after different times of regeneration.

were close to Q_{exp}. As indicated by León et al.,[27] the second-order model proposes a chemisorption process. Even though, this is in good agreement with previously published articles shown in Table S6, where it is demonstrated that the best kinetic model for MP and BP adsorption onto different adsorbents and various experimental conditions followed the pseudo-second-order model.

Additionally, to offer more understanding of the adsorption mechanism and the rate-controlling steps that affect the kinetics, data from dynamic adsorption assays were evaluated using the Weber−Morris intraparticle and Boyd film diffusion models. The results are shown in Figure 6c,6d and Table S4. Remarkably, the Weber−Morris intraparticle diffusion plots were multilinear (Figure 6c,6d), indicating that the adsorption process is a complex process involving surface adsorption, interparticle diffusion, and intraparticle diffusion.[58]

Comparing the three diffusion constants of the Weber−Morris model (Kid.$_1$), it is evidenced that Kid.$_2$ > Kid.$_1$ > Kid.$_3$, as shown in Table S4. Therefore, the second stage is the critical step in the adsorption process of MP and BP on MC, MCB, and MCMM. In fact, this phase refers to the diffusion of molecules to the most internal adsorption sites of the adsorbent being supported by the reduction of the kdif$_3$ value, and this phase has been assigned to the equilibrium stage.[58] Additionally, the first phase or film diffusion was short, in this stage, and the molecules of MP and BP moved through the boundary layer on the surface of the modified cellulose.[59] Moreover, the rise in Ci values (Table S4) was due to the increase in the thickness of the boundary film and the adsorption driving force that were related to the initial concentration of the molecules studied.[27]

Graphs of the Boyd model (Figure 6e,6f) showed that the experimental data did not follow a linear trend and did not pass through (0.0). This proves that the adsorption process for both MP and BP adsorption on MC and MCM was affected by both intraparticle and external diffusion,[58] which supports the results obtained from the Weber and Morris model presented above. However, the film diffusion for the parabens studied on MCB was a minimum.

Adsorption Isotherms. To evaluate the performance of modified cellulose in the removal of methylparaben and butylparaben, adsorption assays were carried out at 20 °C over the time range given by the kinetic experiments. In addition, the experimental data were evaluated using Langmuir, Freundlich, and Sips isotherm models. Figure 7 shows the adsorption isotherms of methylparaben and butylparaben at 20 °C on the modified cellulose evaluated. It is important to note that the adsorption capacity of methylparaben and butylparaben was higher on modified cellulose (MCB and MCM) than that on the source microcrystalline cellulose (MC); moreover, the modified cellulose evaluated had a better adsorption capacity for butylparaben than for methylparaben. This is in good agreement with previous adsorption studies with

https://doi.org/10.1021/acsomega.3c10304
ACS Omega 2024, 9, 30224−30233

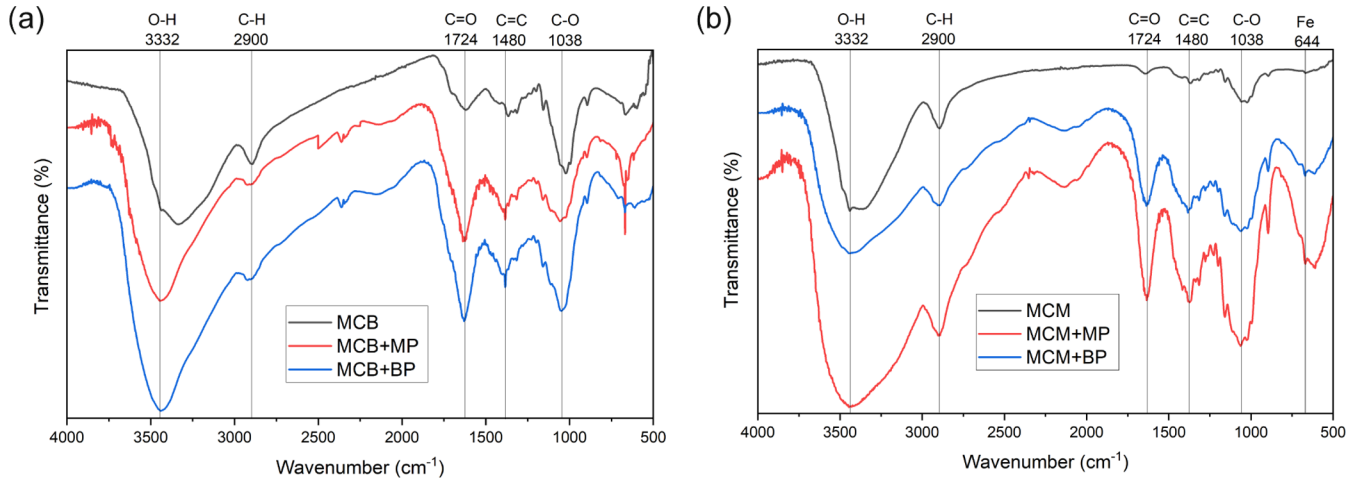

Figure 9. Infrared spectrum of (a) cellulose with benzoic acid (MCB), (b) magnetic cellulose (MCM), and previous and post adsorption of methylparaben (MP) and butylparaben (BP).

parabens, which showed an increase in the adsorption capacity with increasing paraben hydrophobicity. In addition, increasing the molecular size of the substituent group often increases the adsorption capacity, especially for a homologous series of parabens.[16,60] Furthermore, these results offer powerful evidence supported by many authors who argued that the chemical and physical properties of cellulose required for remotion of pollutants depend on molecules worked[19,61,62]

The isotherm parameters for the three isotherm models that worked with linear regression coefficient (R^2) and the sum of the squares of the error (SSE) are listed in Table S5. According to R^2 and SSE, both the Langmuir and the Sips adsorption models could satisfactorily describe the paraben adsorption on each modified cellulose, while the Freundlich isotherm model was the least suitable. This suggests that the adsorption process on modified cellulose implied monolayer adsorption and mixed coverage models.[63] There was a significant positive correlation between our results and those of other paraben-adsorbent complexes employed (Table S6).

Furthermore, the binding constant K_L is associated with the adsorption energy between the adsorbent and the adsorbate.[27] Interestingly, MP showed higher binding constants (MC: 0.2886 L g^{-1}, MCB: 0.1062 L g^{-1}, MCM: 0.2053 L g^{-1}) than BP (MC: 0.1272 L g^{-1}, MCB: 0.0288 L g^{-1}, MCM: 0.1566 L g^{-1}) indicating a higher binding affinity for MP on modified cellulose. In addition, the values of R_L (separation factor) of the Langmuir isotherm were between 0 and 1 at all initial concentrations used for the MP and BP isotherms. Consequently, based on these results, it was determined that the adsorption process was favorable under the conditions used in this study.[64,65]

Our findings appear to be well supported by other research on the removal of MP and BP from aqueous solutions with various adsorbents; this result has been summarized in Table S6. The comparison of the adsorption capacity of modified cellulose (MCB and MCM) with other reported adsorbents was difficult because the condition employed for assays was diverse, but MCB and MCM were better than some adsorbents such as magnetic nanoparticles with a phenyl group,[15] polyacrylonitrile beads,[66] porous N-doped graphene-based NiO composite,[67] β-cyclodextrin-modified mesostructured silica-coated multiwalled carbon nanotube composites,[68] polyamide,[69] and coconut-based activated carbon.[70] In addition, the best adsorbent in our study, MCM, had advantages such as a low amount of adsorbent loading and easy separation of adsorbent using an external magnetic field.

Reuse Cycles of Cellulosic Materials. The cellulosic materials (MCB and MCM) were tested in four cycles for the adsorption of MP and BP under the conditions used in the adsorption isotherm tests. As shown in Figure 8, the adsorption of MP onto MCB and MCM decayed slowly to 20% in the first three cycles. However, the adsorption of BP onto MCM declined slowly to 10% in the first cycle but decreased to about 50% in the second cycle; in addition, the adsorption of BP onto MCB decreased to about 33% in the first cycle and up to 50% in the third cycle. It is interesting to note that the performance of the cellulosic materials depends on the parabens worked, and the reasons for this result are not yet fully understood.

Finally, an adsorption mechanism suggested by us could be that MP and BP molecules were adsorbed mainly through $\pi-\pi$ bonding, hydrogen bonding, n$-\pi$ interactions, and hydrophobic interactions between MP and BP with aromatic and hydroxyl groups on the adsorbent surface of MC and MCB. Additionally, electrostatic interactions could occur between the studied parabens and MCM. This behavior could be seen through the analysis of the infrared spectra previous and after adsorption of the studied pollutants (Figure 9), which showed that signals at 3332, 1724, 1480, and 1128 cm^{-1} changed their position or transmittance intensity increased after the adsorption of parabens. This is in good agreement with previous findings.[71−74] Significantly, further experimental studies are needed to establish the adsorption mechanisms.

CONCLUSIONS

Chemically modified microcellulose with benzoic acid and magnetite (MCB, MCM) was developed for the removal of methylparaben and butylparaben. For both adsorbents, the adsorption capacity of parabens improved with the increase in paraben concentration and enhanced with the molecular mass of the parabens; therefore, butylparaben was adsorbed more than methylparaben, possibly due to its higher hydrophobicity. Additionally, the addition of benzoic acid and magnetite increased the adsorption capacity of parabens due to changes in the surface characteristics of the adsorbents related to the number of functional groups that can interact with the paraben

https://doi.org/10.1021/acsomega.3c10304
ACS Omega 2024, 9, 30224−30233

through hydrogen bridge interactions (oxygenated functional groups), $\pi-\pi$ bonding, and hydrophobic interactions (polyaromatic π-electron functional groups). These increases are more important in the case of magnetite. In conclusion, MCB and MCM were successfully tested as adsorbents for the adsorption of selected methyl and butylparaben compounds. The strength importance of our study was that MCM has a high ability to remove parabens from aqueous solutions; thus, it has potential for possible application in the treatment of polluted effluents.

■ ASSOCIATED CONTENT

Supporting Information

The Supporting Information is available free of charge at https://pubs.acs.org/doi/10.1021/acsomega.3c10304.

Selected physicochemical properties of methylparaben and butylparaben (Table S1); X-ray dispersive spectra (EDX) of microcrystalline cellulose, cellulose with benzoic acid, and magnetic cellulose (Figure S1); magnetic cellulose performance to the external magnetic field (Figure S2); summary of kinetics and isotherm adsorption models used (Table S2); summary of error functions (Table S3); parameters of kinetic model and statistical indices for adsorption of methylparaben and butylparaben onto cellulose evaluated at 20 °C (Table S4); estimated parameters of Langmuir, Freundlich, and Sips isotherm models at 20 °C for adsorption of methylparaben and butylparaben onto cellulose evaluated (Table S5); and maximum adsorption capacity of methylparaben and butylparaben, best isotherm and kinetic models, determined for various adsorbents (Table S6) (PDF)

■ AUTHOR INFORMATION

Corresponding Author

Yaned Milena Correa-Navarro − *Departamento de Química, Facultad de Ciencias Exactas y Naturales, Universidad de Caldas, Manizales 170004 Caldas, Colombia;* orcid.org/0000-0001-9236-209X; Email: yaned.correa@ucaldas.edu.co

Authors

Juan David Rivera-Giraldo − *Departamento de Química, Facultad de Ciencias Exactas y Naturales, Universidad de Caldas, Manizales 170004 Caldas, Colombia;* orcid.org/0000-0003-1335-5620

Julio Andrés Cardona-Castaño − *Departamento de Química, Facultad de Ciencias Exactas y Naturales, Universidad de Caldas, Manizales 170004 Caldas, Colombia;* orcid.org/0000-0003-2990-9480

Complete contact information is available at: https://pubs.acs.org/10.1021/acsomega.3c10304

Notes

The authors declare no competing financial interest.

■ ACKNOWLEDGMENTS

The authors thank the Vice-rectory of Research and Postgraduate of the Universidad de Caldas (Manizales, Colombia) with the program "Convocatoria general de financiación de proyectos de investigación, investigación creación e innovación 2020" number 0312421.

■ REFERENCES

(1) Bolujoko, N. B.; Unuabonah, E. I.; Alfred, M. O.; Ogunlaja, A.; Ogunlaja, O. O.; Omorogie, M. O.; Olukanni, O. D. Toxicity and Removal of Parabens from Water: A Critical Review. *Sci. Total Environ.* **2021**, *792*, No. 148092.

(2) Nowak, K.; Ratajczak-Wrona, W.; Górska, M.; Jabłońska, E. Parabens and Their Effects on the Endocrine System. *Mol. Cell. Endocrinol.* **2018**, *474*, 238−251.

(3) Khezeli, T.; Daneshfar, A.; Kardani, F. In-Situ Functionalization of MnO2 Nanoparticles by Natural Tea Polyphenols: A Greener Sorbent for Dispersive Solid-Phase Extraction of Parabens from Wastewater and Cosmetics. *Microchem. J.* **2023**, *190* (March), No. 108751.

(4) Wei, F.; Mortimer, M.; Cheng, H.; Sang, N.; Guo, L.-H. Parabens as Chemicals of Emerging Concern in the Environment and Humans: A Review. *Sci. Total Environ.* **2021**, *778*, No. 146150.

(5) Meng, Z.; Yu, B.; Chen, Y.; Deng, Y.; Li, H.; Yao, J.; Yang, H. Y. The High Content of NH2-MIL-101(Fe) in NH2-MIL-101(Fe)/Fe3O4/GO Enables Selective Adsorption Removal of Five Parabens. *Chem. Eng. Sci.* **2024**, *284*, No. 119527.

(6) Ocaña-González, J. A.; Villar-Navarro, M.; Ramos-Payán, M.; Fernández-Torres, R.; Bello-López, M. A. New Developments in the Extraction and Determination of Parabens in Cosmetics and Environmental Samples. A Review. *Anal. Chim. Acta* **2015**, *858*, 1−15.

(7) Monneret, C. What Is an Endocrine Disruptor? *C. R. Biol.* **2017**, *340* (9), 403−405.

(8) Maia, C.; Sousa, C. A.; Sousa, H.; Vale, F.; Simões, M. Parabens Removal from Wastewaters by Microalgae − Ecotoxicity, Metabolism and Pathways. *Chem. Eng. J.* **2023**, *453*, No. 139631.

(9) Kabir, E. R.; Rahman, M. S.; Rahman, I. A Review on Endocrine Disruptors and Their Possible Impacts on Human Health. *Environ. Toxicol. Pharmacol.* **2015**, *40* (1), 241−258.

(10) Tartaglia, A.; Kabir, A.; Ulusoy, S.; Sperandio, E.; Piccolantonio, S.; Ulusoy, H. I.; Furton, K. G.; Locatelli, M. FPSE-HPLC-PDA Analysis of Seven Paraben Residues in Human Whole Blood, Plasma, and Urine. *J. Chromatogr. B* **2019**, *1125*, No. 121707.

(11) Smarr, M. M.; Sundaram, R.; Honda, M.; Kannan, K.; Louis, G. M. B. Urinary Concentrations of Parabens and Other Antimicrobial Chemicals and Their Association with Couples' Fecundity. *Environ. Health Perspect.* **2017**, *125* (4), 730−736.

(12) Darbre, P. D.; Aljarrah, A.; Miller, W. R.; Coldham, N. G.; Sauer, M. J.; Pope, G. S. Concentrations of Parabens in Human Breast Tumours. *J. Appl. Toxicol.* **2004**, *24* (1), 5−13.

(13) Amin, M. M.; Hashemi, M.; Ebrahimpour, K.; Chavoshani, A. Determination of Parabens in Wastewater and Sludge in a Municipal Wastewater Treatment Plant Using Microwaveassisted Dispersive Liquid-Liquid Microextraction Coupled with Gas Chromatography-Mass Spectrometry. *Environ. Health Eng. Manag.* **2019**, *6* (3), 215−224.

(14) INVIMA. Resolución No 1905. Por La Que Se Prohíbe El Uso de Los Parabenos de Cadena Larga Como Ingredientes Para Productos Cosméticos En La Comunidad Andina, 2017, pp 1−2.

(15) Chen, H. W.; Chiou, C. S.; Chang, S. H. Comparison of Methylparaben, Ethylparaben and Propylparaben Adsorption onto Magnetic Nanoparticles with Phenyl Group. *Powder Technol.* **2017**, *311*, 426−431.

(16) De Oliveira, F. F.; Moura, K. O.; Costa, L. S.; Vidal, C. B.; Loiola, A. R.; Do Nascimento, R. F. Reactive Adsorption of Parabens on Synthesized Micro- And Mesoporous Silica from Coal Fly Ash: PH Effect on the Modification Process. *ACS Omega* **2020**, *5* (7), 3346−3357.

(17) Hokkanen, S.; Bhatnagar, A.; Sillanpää, M. A Review on Modification Methods to Cellulose-Based Adsorbents to Improve Adsorption Capacity. *Water Res.* **2016**, *91*, 156−173.

(18) Gupta, A.; Ladino, C. R.; Mekonnen, T. H. Cationic Modification of Cellulose as a Sustainable and Recyclable Adsorbent for Anionic Dyes. *Int. J. Biol. Macromol.* **2023**, *234*, No. 123523.

(19) Abdelhamid, H. N.; Mathew, A. P. Cellulose-Based Materials for Water Remediation: Adsorption, Catalysis, and Antifouling. *Front. Chem. Eng.* **2021**, *3*, 1−23.
(20) Periyasamy, S.; Gopalakannan, V.; Viswanathan, N. Fabrication of Magnetic Particles Imprinted Cellulose Based Biocomposites for Chromium(VI) Removal. *Carbohydr. Polym.* **2017**, *174*, 352−359.
(21) Espino-Pérez, E.; Domenek, S.; Belgacem, N.; Sillard, C.; Bras, J. Green Process for Chemical Functionalization of Nanocellulose with Carboxylic Acids. *Biomacromolecules* **2014**, *15* (12), 4551−4560.
(22) Periyasamy, S.; Gopalakannan, V.; Viswanathan, N. Enhanced Chromium Sorption and Quick Separation of Magnetic Hydrotalcite Anchored Biopolymeric Composites Using the Hydrothermal Method. *J. Chem. Eng. Data* **2018**, *63* (5), 1286−1299.
(23) Yu, Z.; Hu, C.; Dichiara, A. B.; Jiang, W.; Gu, J. Cellulose Nanofibril/Carbon Nanomaterial Hybrid Aerogels for Adsorption Removal of Cationic and Anionic Organic Dyes. *Nanomaterials* **2020**, *10* (1), 1−20.
(24) Ruan, C.; Ma, Y.; Shi, G.; He, C.; Du, C.; Jin, X.; Liu, X.; He, S.; Huang, Y. Self-Assembly Cellulose Nanocrystals/SiO2 Composite Aerogel under Freeze-Drying: Adsorption towards Dye Contaminant. *Appl. Surf. Sci.* **2022**, *592*, No. 153280.
(25) Shojaeiarani, J.; Bajwa, D. S.; Stark, N. M. Green Esterification: A New Approach to Improve Thermal and Mechanical Properties of Poly(Lactic Acid) Composites Reinforced by Cellulose Nanocrystals. *J. Appl. Polym. Sci.* **2018**, *135* (27), 1−8.
(26) Moreno-Marenco, A. R.; Giraldo, L.; Moreno-Piraján, J. C. Adsorption of N-Butylparaben from Aqueous Solution on Surface of Modified Granular Activated Carbons Prepared from African Palm Shell. Thermodynamic Study of Interactions. *J. Environ. Chem. Eng.* **2020**, *8* (4), No. 103969.
(27) León, G.; Hidalgo, A. M.; Martínez, A.; Guzmán, M. A.; Miguel, B. Methylparaben Adsorption onto Activated Carbon and Activated Olive Stones: Comparative Analysis of Efficiency, Equilibrium, Kinetics and Effect of Graphene-Based Nanomaterials Addition. *Appl. Sci.* **2023**, *13* (16), 9147.
(28) Singh, V.; Srivastava, V. C. Self-Engineered Iron Oxide Nanoparticle Incorporated on Mesoporous Biochar Derived from Textile Mill Sludge for the Removal of an Emerging Pharmaceutical Pollutant. *Environ. Pollut.* **2020**, *259*, No. 113822.
(29) Marahel, F.; Mombeeni Goodajdar, B.; Basari, N.; Niknam, L.; Ghazali, A. A. Applying Neural Network Model for Adsorption Methyl Paraben (MP) Dye Using Ricinus Communis-Capeed Fe3O4 NPs Synthesized from Aqueous Solution. *Iran. J. Chem. Chem. Eng.* **2022**, *41* (7), 2358−2377.
(30) Abushammala, H.; Mao, J. A Review of the Surface Modification of Cellulose and Nanocellulose Using Aliphatic and Aromatic Mono- and Di-Isocyanates. *Molecules* **2019**, *24* (15), 2782.
(31) Fraschini, C.; Chauve, G.; Bouchard, J. TEMPO-Mediated Surface Oxidation of Cellulose Nanocrystals (CNCs). *Cellulose* **2017**, *24* (7), 2775−2790.
(32) Wu, Z.; Xu, J.; Gong, J.; Li, J.; Mo, L. Preparation, Characterization and Acetylation of Cellulose Nanocrystal Allomorphs. *Cellulose* **2018**, *25* (9), 4905−4918.
(33) Wang, Y.; Wang, X.; Xie, Y.; Zhang, K. Functional Nanomaterials through Esterification of Cellulose: A Review of Chemistry and Application. *Cellulose* **2018**, *25* (7), 3703−3731.
(34) Zhou, L.; Ke, K.; Yang, M. B.; Yang, W. Recent Progress on Chemical Modification of Cellulose for High Mechanical-Performance Poly(Lactic Acid)/Cellulose Composite: A Review. *Compos. Commun.* **2021**, *23*, No. 100548.
(35) HPS, A. K.; Saurabh, C. K.; AS, A.; Nurul Fazita, M. R.; Syakir, M. I.; Davoudpour, Y.; Rafatullah, M.; Abdullah, C. K.; Haafiz, M. K. M.; Dungani, R. A Review on Chitosan-Cellulose Blends and Nanocellulose Reinforced Chitosan Biocomposites: Properties and Their Applications. *Carbohydr. Polym.* **2016**, *150*, 216−226.
(36) Olivera, S.; Muralidhara, H. B.; Venkatesh, K.; Guna, V. K.; Gopalakrishna, K.; Kumar, K. Y. Potential Applications of Cellulose and Chitosan Nanoparticles/Composites in Wastewater Treatment: A Review. *Carbohydr. Polym.* **2016**, *153*, 600−618.
(37) Patel, D. K.; Dutta, S. D.; Lim, K.-T. Nanocellulose-Based Polymer Hybrids and Their Emerging Applications in Biomedical Engineering and Water Purification. *RSC Adv.* **2019**, *9* (33), 19143−19162.
(38) Aguilar-Sanchez, A.; Jalvo, B.; Mautner, A.; Rissanen, V.; Kontturi, K. S.; Abdelhamid, H. N.; Tammelin, T.; Mathew, A. P. Charged Ultrafiltration Membranes Based on TEMPO-Oxidized Cellulose Nanofibrils/Poly(Vinyl Alcohol) Antifouling Coating. *RSC Adv.* **2021**, *11* (12), 6859−6868.
(39) Dong, Y.-D.; Zhang, H.; Zhong, G.-J.; Yao, G.; Lai, B. Cellulose/Carbon Composites and Their Applications in Water Treatment − a Review. *Chem. Eng. J.* **2021**, *405*, No. 126980.
(40) Miyashiro, D.; Hamano, R.; Umemura, K. A Review of Applications Using Mixed Materials of Cellulose, Nanocellulose and Carbon Nanotubes. *Nanomaterials* **2020**, *10* (2), 186.
(41) Soliman, M.; Sadek, A. A.; Abdelhamid, H. N.; Hussein, K. Graphene Oxide-Cellulose Nanocomposite Accelerates Skin Wound Healing. *Res. Vet. Sci.* **2021**, *137*, 262−273.
(42) Farooq, A.; Patoary, M. K.; Zhang, M.; Mussana, H.; Li, M.; Naeem, M. A.; Mushtaq, M.; Farooq, A.; Liu, L. Cellulose from Sources to Nanocellulose and an Overview of Synthesis and Properties of Nanocellulose/Zinc Oxide Nanocomposite Materials. *Int. J. Biol. Macromol.* **2020**, *154*, 1050−1073.
(43) Oyewo, O. A.; Mutesse, B.; Leswifi, T. Y.; Onyango, M. S. Highly Efficient Removal of Nickel and Cadmium from Water Using Sawdust-Derived Cellulose Nanocrystals. *J. Environ. Chem. Eng.* **2019**, *7* (4), No. 103251.
(44) Baghdad, K.; Hasnaoui, A. M. Zeolite−Cellulose Composite Membranes: Synthesis and Applications in Metals and Bacteria Removal. *J. Environ. Chem. Eng.* **2020**, *8* (4), No. 104047.
(45) Abdelhamid, H. N.; Mathew, A. P. Cellulose−Metal Organic Frameworks (CelloMOFs) Hybrid Materials and Their Multifaceted Applications: A Review. *Coord. Chem. Rev.* **2022**, *451*, No. 214263.
(46) Abdelhamid, H. N.; Mathew, A. P. In-Situ Growth of Zeolitic Imidazolate Frameworks into a Cellulosic Filter Paper for the Reduction of 4-Nitrophenol. *Carbohydr. Polym.* **2021**, *274*, No. 118657.
(47) Al-Musawi, T. J.; Mengelizadeh, N.; Al Rawi, O.; Balarak, D. Capacity and Modeling of Acid Blue 113 Dye Adsorption onto Chitosan Magnetized by Fe2O3 Nanoparticles. *J. Polym. Environ.* **2022**, *30* (1), 344−359.
(48) Beroual, M.; Boumaza, L.; Mehelli, O.; Trache, D.; Tarchoun, A. F.; Khimeche, K. Physicochemical Properties and Thermal Stability of Microcrystalline Cellulose Isolated from Esparto Grass Using Different Delignification Approaches. *J. Polym. Environ.* **2021**, *29* (1), 130−142.
(49) Rathinavelu, R.; Paramathma, B. S.; Divkaran, D.; Siengchin, S. Physicochemical, Thermal, and Morphological Properties of Microcrystalline Cellulose Extracted from Calotropis Gigantea Leaf. *Biomass Convers. Biorefin.* **2023**, *0123456789*, 1−18.
(50) Zirak, M.; Abdollahiyan, A.; Eftekhari-Sis, B.; Saraei, M. Carboxymethyl Cellulose Coated Fe3O4@SiO2 Core−Shell Magnetic Nanoparticles for Methylene Blue Removal: Equilibrium, Kinetic, and Thermodynamic Studies. *Cellulose* **2018**, *25* (1), 503−515.
(51) Van, N. T. T.; Phan, A. N.; Cuong, V. C.; Van, N. T. T.; Thanh, H. G.-T.; Khai, N. Q.; Tri, N.; Nguyen, T.-T.; Bui, X.-T.; Huynh, K. P. H. Enhanced Heterogeneous Fenton Degradation of P-Nitrophenol by Fe3O4 Nanoparticles Decorated Cellulose Aerogel from Banana Stem. *Environ. Technol. Innovation* **2023**, *30*, No. 103041.
(52) Chen, X.; Chen, X.; Cai, X. M.; Huang, S.; Wang, F. Cellulose Dissolution in a Mixed Solvent of Tetra(n-Butyl)Ammonium Hydroxide/Dimethyl Sulfoxide via Radical Reactions. *ACS Sustainable Chem. Eng.* **2018**, *6* (3), 2898−2904.
(53) Janićijević, A.; Pavlović, V. P.; Kovačević, D.; Perić, M.; Vlahović, B.; Pavlović, V. B.; Filipović, S. Structural Characterization of Nanocellulose/Fe3O4 Hybrid Nanomaterials. *Polymers* **2022**, *14* (9), 1819.

https://doi.org/10.1021/acsomega.3c10304
ACS Omega 2024, 9, 30224−30233

(54) Yusoff, M. M.; Yahaya, N.; Saleh, N. M.; Raoov, M. A Study on the Removal of Propyl, Butyl, and Benzyl Parabens: Via Newly Synthesised Ionic Liquid Loaded Magnetically Confined Polymeric Mesoporous Adsorbent. *RSC Adv.* **2018**, *8* (45), 25617−25635.
(55) Chen, H.-W.; Chiou, C.-S.; Chang, S.-H. Comparison of Methylparaben, Ethylparaben and Propylparaben Adsorption onto Magnetic Nanoparticles with Phenyl Group. *Powder Technol.* **2017**, *311*, 426−431.
(56) Li, K.; Yang, H.; Jiang, L.; Liu, X.; Lang, P.; Deng, B.; Li, N.; Xu, W. Glycerin/NaOH Aqueous Solution as a Green Solvent System for Dissolution of Cellulose. *Polymers* **2020**, *12* (8), 1−11.
(57) Yue, Y. *A Comparative Study of Cellulose I and II and Fibers and Nanocrystals*; Louisiana State University and Agricultural & Mechanical College, 2011.
(58) Campos, N. F.; Barbosa, C. M. B. M.; Rodríguez-Díaz, J. M.; Duarte, M. M. M. Removal of Naphthenic Acids Using Activated Charcoal: Kinetic and Equilibrium Studies. *Adsorpt. Sci. Technol.* **2018**, *36*, 2−17.
(59) Lian, Q.; Yao, L.; Uddin Ahmad, Z.; Gang, D. D.; Konggidinata, M. I.; Gallo, A. A.; Zappi, M. E. Enhanced Pb(II) Adsorption onto Functionalized Ordered Mesoporous Carbon (OMC) from Aqueous Solutions: The Important Role of Surface Property and Adsorption Mechanism. *Environ. Sci. Pollut. Res.* **2020**, *27* (19), 23616−23630.
(60) Yusoff, M. M.; Yahaya, N.; Saleh, N. M.; Raoov, M. A Study on the Removal of Propyl, Butyl, and Benzyl Parabens: Via Newly Synthesised Ionic Liquid Loaded Magnetically Confined Polymeric Mesoporous Adsorbent. *RSC Adv.* **2018**, *8* (45), 25617−25635.
(61) Agustin, M. B.; Mikkonen, K. S.; Kemell, M.; Lahtinen, P.; Lehtonen, M. Systematic Investigation of the Adsorption Potential of Lignin- and Cellulose-Based Nanomaterials towards Pharmaceuticals. *Environ. Sci. Nano* **2022**, *9* (6), 2006−2019.
(62) Du, L.; Wang, J.; Zhang, Y.; Qi, C.; Wolcott, M. P.; Yu, Z. Preparation and Characterization of Cellulose Nanocrystals from the Bio-Ethanol Residuals. *Nanomaterials* **2017**, *7* (3), 1−12.
(63) Xu, C.; Yu, T.; Peng, J.; Zhao, L.; Li, J.; Zhai, M. Efficient Adsorption Performance of Lithium Ion onto Cellulose Microspheres with Sulfonic Acid Groups. *Quantum Beam Sci.* **2020**, *4* (1), 6.
(64) Al-Ghouti, M. A.; Da'ana, D. A. Guidelines for the Use and Interpretation of Adsorption Isotherm Models: A Review. *J. Hazard. Mater.* **2020**, *393*, No. 122383.
(65) Ayawei, N.; Ebelegi, A. N.; Wankasi, D. Modelling and Interpretation of Adsorption Isotherms. *J. Chem.* **2017**, *2017*, 1−11.
(66) Forte, M.; Mita, L.; Perrone, R.; Rossi, S.; Argirò, M.; Mita, D. G.; Guida, M.; Portaccio, M.; Godievargova, T.; Ivanov, Y.; et al. Removal of Methylparaben from Synthetic Aqueous Solutions Using Polyacrylonitrile Beads: Kinetic and Equilibrium Studies. *Environ. Sci. Pollut. Res.* **2017**, *24* (2), 1270−1282.
(67) Husein, D. Z. Facile One-Pot Synthesis of Porous N-Doped Graphene Based NiO Composite for Parabens Removal from Wastewater and Its Reusability. *Desalin. Water Treat.* **2019**, *166*, 211−221.
(68) Ding, C.; He, J.; Xu, M.; Wang, C. Fabrication of *β*-Cyclodextrin Modified Mesostructured Silica Coated Multi-Walled Carbon Nanotubes Composites and Application for Paraben Removal. *Water Sci. Technol.* **2018**, *78* (5), 1001−1009.
(69) Mejías, C.; Martín, J.; Santos, J. L.; Aparicio, I.; Alonso, E. Role of Polyamide Microplastics as Vector of Parabens in the Environment: An Adsorption Study. *Environ. Technol. Innovation* **2023**, *32*, No. 103276.
(70) Atheba, P.; Allou, N. B.; Drogui, P.; Trokourey, A. Adsorption Kinetics and Thermodynamics of ADN on Activated Carbon. *J. Encapsulation Adsorpt. Sci.* **2018**, *8*, 39−57.
(71) Chen, H. W.; Chiou, C. S.; Wu, Y. P.; Chang, C. H.; Lai, Y. H. Magnetic Nanoadsorbents Derived from Magnetite and Graphene Oxide for Simultaneous Adsorption of Nickel Ion, Methylparaben, and Reactive Black 5. *Desalin. Water Treat.* **2021**, *224*, 168−177.
(72) Ran, J.; Li, M.; Zhang, C.; Xue, F.; Tao, M.; Zhang, W. Synergistic Adsorption for Parabens by an Amphiphilic Functionalized Polypropylene Fiber with Tunable Surface Microenvironment. *ACS Omega* **2020**, *5* (6), 2920−2930.
(73) Mashile, G. P.; Mpupa, A.; Nqombolo, A.; Dimpe, K. M.; Nomngongo, P. N. Recyclable Magnetic Waste Tyre Activated Carbon-Chitosan Composite as an Effective Adsorbent Rapid and Simultaneous Removal of Methylparaben and Propylparaben from Aqueous Solution and Wastewater. *J. Water Process Eng.* **2020**, *33*, No. 101011.
(74) Nodeh, H. R.; Sereshti, H.; Ataolahi, S.; Toloutehrani, A.; Ramezani, A. T. Activated Carbon Derived from Pistachio Hull Biomass for the Effective Removal of Parabens from Aqueous Solutions: Isotherms, Kinetics, and Free Energy Studies. *Desalin. Water Treat.* **2020**, *201*, 155−164.

https://doi.org/10.1021/acsomega.3c10304
ACS Omega 2024, 9, 30224−30233